

The Lunar Radio Array (LRA)

Joseph Lazio (NRL), C. Carilli (NRAO), J. Hewitt (MIT), S. Furlanetto (UCLA),
& J. Burns (Colorado), for the LUNAR Consortium

ABSTRACT

The Lunar Radio Array (LRA) is a concept for a telescope sited on the farside of the Moon with a prime mission of making precision cosmological measurements via observations of neutral hydrogen.

The Dark Ages represent one of the last frontiers in cosmology, the era between the genesis of the CMB at recombination and the formation of the first stars. During the Dark Ages—when the Universe was unlit by stars—and into the Epoch of Reionization (EoR), there is likely to be a detectable signal from neutral hydrogen (H I) in the intergalactic medium (IGM). This H I signal represents potentially the richest of all cosmological data and also can provide crucial information about the epoch of the first stars that initiate the EoR and the role of the first black holes in heating the IGM. The farside of the Moon is likely the only site in the inner solar system for exploiting this potential fully as significant obstacles exist to ground-based telescopes, including heavy use of the relevant portion of the spectrum by both civil and military transmitters and distortions introduced by the Earth's ionosphere.

Technology development over the next decade is needed to enable the deployment of the LRA in following decades. I illustrate notional LRA concepts and discuss required technologies, with a particular focus on those having a broad applicability to missions other than the LRA.

1 COSMOLOGY & ASTROPHYSICS WITH THE HIGHLY-REDSHIFTED 21-CM LINE

Modern cosmology has advanced rapidly in recent years owing to precision observations of the cosmic microwave background (CMB)⁷; large data sets produced by wide field galaxy surveys (2dFGRS⁴, SDSS⁵); and observations of Type Ia supernovae.^{10,12} This information has produced a standard model for cosmology. Yet significant questions remain

- **Does the standard cosmological model describe the universe during the “Dark Ages,” before the first stars formed?**
- **How does the IGM evolve during this important time, ending with the reionization of hydrogen?**
- **What were the properties of high- z galaxies? How did they affect the Universe around them?**
- **What is the nature of the field that drove the universe during inflation?**

Hydrogen is the dominant component of the IGM, and neutral hydrogen (H I) displays a hyperfine spin-flip transition at a frequency of 1420 MHz. The feasibility of observing this redshifted H I line has stirred significant recent interest because it offers the chance to extend current data sets by orders of magnitude^{6,9}. Through detailed mapping of the H I line brightness temperature in space and frequency, it might be possible to determine the distribution of hydrogen throughout the Universe from the present day to a redshift $z \sim 100$. This unprecedented data set would constrain the properties of the inflation era, detect signatures of any exotic heating mechanisms before the first star formation (e.g., dark matter decay), and constrain the properties of “dark energy” and fundamental gravity by tracking the evolution of the angular scale of the baryon acoustic oscillations. It would also provide a wealth of astrophysical data on the first galaxies and their descendants, including the properties of the first stars and the birth of the first black holes.

Figure 1 shows the evolution of the global (all-sky averaged) H I signal after recombination; shown are the signals in three models chosen so that the astrophysical parameters yield a CMB optical depth to electron scattering of $\tau = 0.06$, 0.09, and 0.12, corresponding to the WMAP5 central and $\pm 2\sigma$ values. Three regimes are apparent. At high redshifts ($30 < z < 300$), collisions in the gas produce a broad absorption signal because the gas expands and cools at a faster rate than the CMB; this signal fades as the Universe continues to expand and collisions become more rare. Once the first stars form, they flood the Universe with Ly α photons, which produce a second, deep absorption feature ($15 < z < 30$). Finally, as the gas is heated above the CMB temperature (probably by X-rays from the first black holes), the absorption turns into emission, which eventually cuts off as reionization completes.

This global signature is currently an experimental target.² Although conceptually simple, these observations are experimentally challenging, because of the difficulty of separating the faint signal from the many other sources of emission, including Galactic synchrotron, free-free radiation, and the CMB as well as corrupting effects due to observing

from the ground (§2). Experimental detection relies upon a distinctive, step-like feature in frequency (Figure 1, left), which is not expected from the spectrally smooth foregrounds; current limits are an order of magnitude short of theoretical expectations.

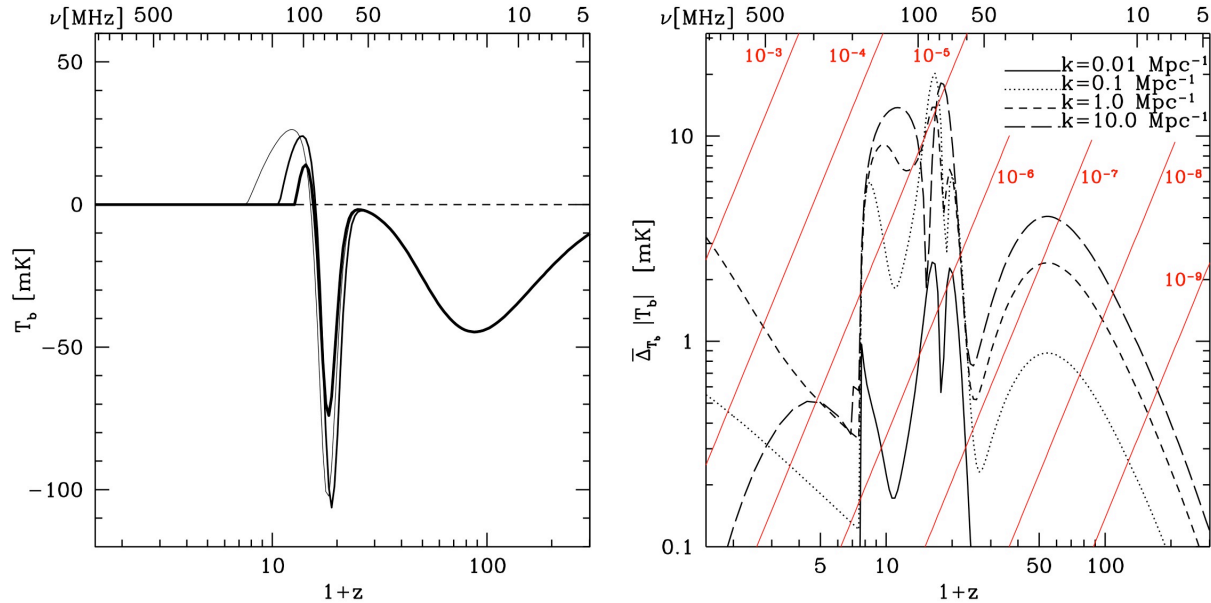


Figure 1. (Left) Evolution of the mean H I line brightness temperature T_b as a function of redshift (bottom axis) or frequency (top axis) for three models of the first galaxies representing the range of astrophysical parameters consistent with CMB analyses.¹¹ **(Right)** Redshift (frequency) evolution in one model for the angle-averaged H I line power spectrum Δ_T at $k = 0.01$ (solid curve), 0.1 (dotted), 1.0 (short dashed), and 10.0 (long dashed) Mpc^{-1} . Reionization occurs at $z = 6.5$. Diagonal red lines show the strength of the combination of Galactic and extragalactic foregrounds reduced by indicated numerical factors.

An alternate, and ultimately more powerful, approach is through H I line fluctuations, conventionally parameterized with the power spectrum. Figure 1 (right) illustrates the redshift (frequency) evolution of the power spectrum $\Delta_T \equiv (k^3 P_T(k)/2\pi^2)^{1/2}$ at four comoving wavenumbers $k = 0.01, 0.1, 1,$ and 10 Mpc^{-1} . These wavenumbers span the range that might be observed: on small wavenumbers (large scales) we expect contamination from foregrounds to limit the detection of the power spectrum, while at large wavenumbers (small scales) thermal broadening of the H I line will smooth the signal.

The shape and amplitude of power spectra encode a great deal of information about the first sources of light and the processes modifying the IGM, and extracting the power spectra at different redshifts will allow the evolution of the IGM to be traced. Figure 2 shows model H I line fluctuation spectra at three different epochs; at $z = 15.7$, the dip at moderate k indicates that X-rays from the first black holes are beginning to heat the IGM, transforming the signal to emission. H I line fluctuation spectra have the potential to distinguish between heating and ionizing sources (i.e., black holes and stars), determine the epoch(s) at which each became important, and constrain the properties of the first galaxies.

This power spectrum approach motivates a number of current generation instruments: the Murchison Wide-field Array (MWA),¹ the Precision Array to Probe the Epoch of Reionization (PAPER),² and the Low Frequency Array (LOFAR),³ all of which focus on detecting the H I power spectrum at redshifts $z \approx 7$, at which the reionization of the neutral IGM produces a large signal. While not directly motivated by EoR observations, the Long Wavelength Array (LWA)⁴ has

¹ MWA: <http://www.mwatelescope.org/>

² PAPER: <http://astro.berkeley.edu/%7Edbacker/eor/>

³ LOFAR: <http://www.lofar.org/>

⁴ LWA: <http://lwa.unm.edu/>

frequency coverage that overlaps with some of these instruments. These pathfinder telescopes will likely be followed by the Square Kilometre Array (SKA)⁵ to perform even more sensitive measurements.

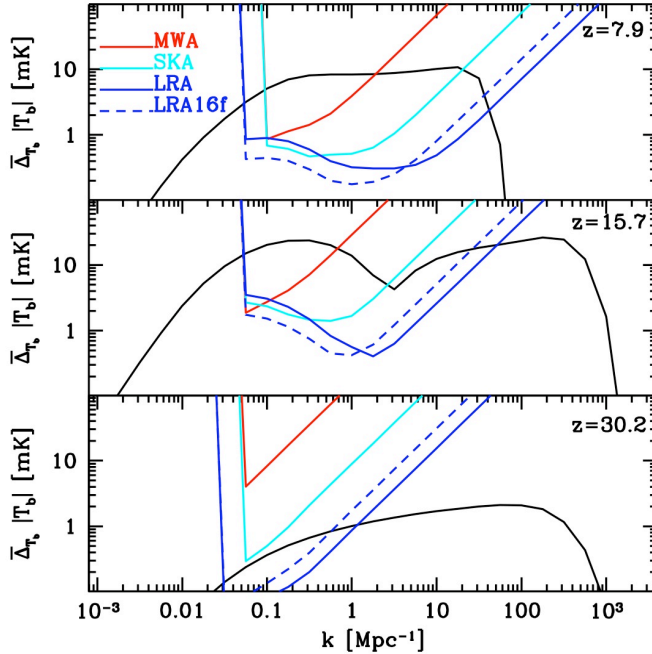


Figure 2. Redshift slices of the H I line power spectrum, for one of the models in Figure 1: during the EoR ($z = 7.9$), during the transition phase ($z = 15.7$), and during the Dark Ages ($z = 30.2$). Also shown are the expected errors for three fiducial instruments, the MWA (red), the SKA (cyan), and a potential LRA (blue); the sensitivity of the LRA is also shown with its observing time split between 16 separate fields (blue dashed).

Foreground removal must be accomplished at a high level of precision for detection of the H I signal. Figure 1 (right) also shows $rT_{\text{sky}}(\nu)$, for $r = 10^{-4}$ – 10^{-9} , with T_{sky} corresponding to the sum of the Galactic non-thermal emission in a dark region of the sky and extragalactic contributions. Lending confidence to the notion of high-precision foreground removal is that the foregrounds are generally *spectrally smooth*, while the H I signal has frequency structure. Further, exotic physics (e.g., energy injection by decaying dark matter⁶) can increase the H I signal strength and reduce the level to which foregrounds need to be removed.

Figure 2 shows redshift slices, and signal-to-noise ratios, for the H I power spectrum for one of the models in Figure 1 at three fiducial epochs: during the EoR, during the transition phase, and during the Dark Ages. Signal-to-noise ratios are shown for three fiducial experiments: (i) a current generation experiment; (ii) the SKA; and (iii) an LRA concept (collecting area $\sim 3.6 \text{ km}^2$, 4-yr observing campaign). These labels primarily denote different scales of experimental effort, as the design for any array following the pathfinders will clearly be informed by their results. Clearly, though the current generation of instruments may detect the EoR H I signal, measuring detailed physics will require efforts comparable to the SKA, which also sets a target for the LRA.

2 THE MOON AS AN ASTRONOMICAL AND COSMOLOGICAL PLATFORM

The lunar *farside* is potentially the only site in the inner solar system for the LRA:

No Human-generated Interference: Civil and military transmitters make heavy use of the relevant frequencies ($\nu < 100 \text{ MHz}$). The FM radio band is at 88–107 MHz, and Digital TV channels and myriad other signals also exist in this frequency range. Further, because of ionospheric refraction, interference in the HF band ($\nu < 30 \text{ MHz}$) used for international communication is independent of location on Earth. Terrestrial transmitters can be orders of magnitude ($\sim 10^{12}$) stronger than the H I signals and are detectable even at remote locations on Earth (Figure 3). The Moon reduces such interference to a negligible level.¹

No (Permanent) Ionosphere: The Earth's ionosphere produces phase errors that limit radio observations (in addition to simply reflecting interference from distant transmitters, Figure 3). These phase errors form a significant fraction of the error budget in the recent 74-MHz VLA Low frequency Sky Survey,³ even after the development of new algorithms for

⁵ SKA: <http://www.skatelescope.org/>

Lunar Radio Array

ionospheric mitigation. While the Moon has a plasma layer due to solar irradiation during the lunar day, this ionized layer disappears during lunar night.

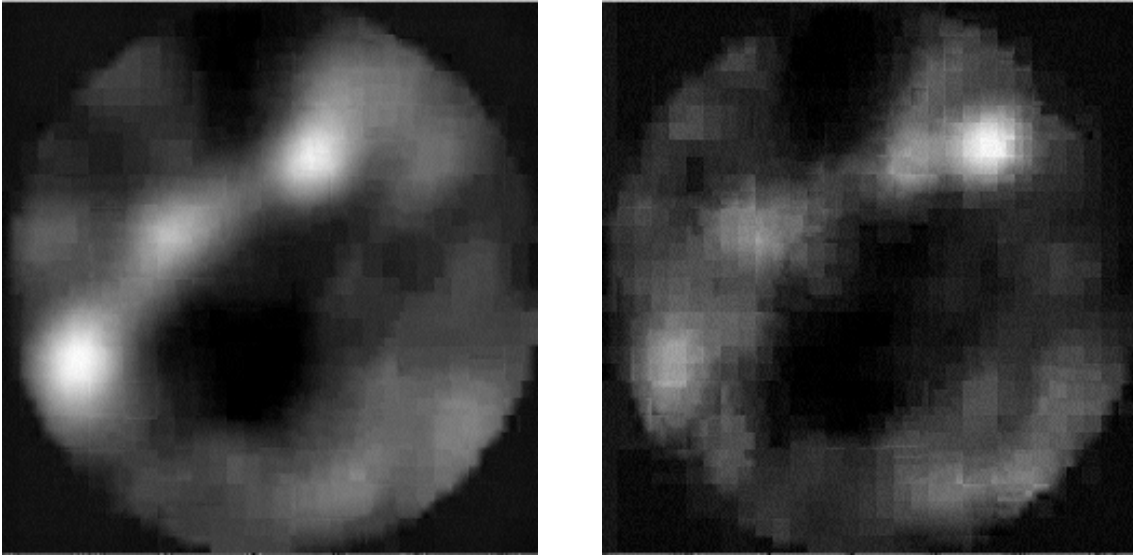


Figure 3. Radio interference enabled by the Earth's atmosphere. (Left) An all-sky, 61-MHz image from the Long Wavelength Demonstrator Array in New Mexico. The Galactic plane slopes from the upper right to the lower left and the sources Cyg A and Cas A are visible as is a general enhancement toward the inner Galaxy. **(Right)** An image acquired seconds later. The dominant source (upper right) is a reflection off an ionized meteor trail from a TV station hundreds of kilometers away. The highest sensitivity astronomical observations will require shielding from such interference, *shielding that can be obtained only on the Moon.*

Shielding from Solar Radio Emission: The Sun is the strongest celestial source at these frequencies when it is bursting. Within the solar system, the only mitigation for solar radio emissions is physical shielding. Such shielding is readily accomplished by observing during lunar night; while the same is true for the surface of the Earth, interference and ionospheric effects continue to occur during terrestrial night.

3 MISSION DESCRIPTION

Tables 1 and 2 summarize key scientific requirements, and derived technical requirements, for the LRA. Depending upon the results from ground-based arrays and the cost-performance achieved, different scientific goals are envisioned. A “nominal” LRA has modest overlap with the redshift range of ground-based arrays and its redshift coverage extends back to the epoch of the first star formation; a “dark ages” LRA has considerable overlap with the redshift range of ground-based arrays and its redshift coverage extends well into the Dark Ages.

Table 1. LRA Scientific Requirements

Parameter	Nominal LRA	Dark Ages LRA
Redshift	8.5–30	6–50
Brightness Temperature Sensitivity	10 mK	4 mK
Angular Resolution	3'	1.4'

The LRA concept draws on the considerable experience from ground-based radio arrays. Multiple radio-receiving elements are operated together to collect radio signals from a particular region of the sky. In the LRA, each array element is composed of a multiple antennas. The individual antenna signals are aligned in time and summed, so that each element behaves as a single very sensitive antenna. The signals from each pair of elements are correlated with one another as an interferometer, and the different baselines between the various pairs sample the brightness distributions across the region of interest.

Table 2. LRA Derived Technical Requirements

Parameter	Nominal LRA	Dark Ages LRA	Scientific Driver / Technology
Collecting Area	0.36 km ²	3 km ²	Brightness Temperature Sensitivity Low-mass antennas
Frequency	50–150 MHz	30–200 MHz	Redshift Electronics, Power
Maximum Baseline	5 km	10 km	Angular Resolution Rovers, Data transport
Lifetime	3 yr	5 yr	Brightness Temperature Sensitivity Power

Two concepts are currently being explored for the LRA—the Dark Ages Lunar Interferometer (DALI, §3.2) and the Lunar Array for Radio Cosmology (LARC, §3.3). Common to both concepts is that, once deployed, the LRA would have no moving parts. Individual aspects of both concepts are described further below. However, both concepts also share a number of common aspects. Command and control information and clock data must be transmitted to the elements from the central station. Digitized, filtered, frequency divided, multiple polarization science data are returned to the central processor and those signals are combined. Data are either correlated real-time and stored at the central processing unit, or stored at the elements and transmitted and correlated during the lunar day.

The LRA will be located on the lunar farside, in a relatively flat area at least 10 km across. A nominal location is the Tsiolkovsky crater, which has been filled in by basaltic mare deposits making its floor relatively flat. LRA components will be delivered to the lunar farside using a heavy-lift vehicle (e.g., Ares V or similar) and lander (e.g., Altair cargo lander or similar). Unpacking, antenna distribution, antenna deployment, and array connection will be handled by rovers, such as the All-Terrain Hex-Legged Extra Terrestrial Explorer (ATHLETE). A central processing unit will remain on the lander and will serve as a control and communications center.

3.1 Technology Development

Table 3 summarizes key technologies that have to be developed for the LRA along with heritage, trade studies, and potential synergies with other Government agencies. Technology relevant to the LRA consists both of technologies specific to the LRA (e.g., low-mass science antennas) as well as technology relevant more broadly (e.g., ultra-low power digital electronics).

Low-frequency, wide-bandwidth, low-mass science antennas: One low-mass science antenna concept (polyimide-film based dipoles) has already been tested in the field (at NASA/GSFC) under the Astrophysics Strategic Mission Concept Studies program. Work by the LUNAR NLSI team budgets a 4-year development and test program (starting in mid-FY09), including electromagnetic simulations, field testing, and thermal-vac chamber testing. This time scale is also comparable to that for the development of new, broadband antennas for the ground-based radio arrays.

Ultra-low power, radiation tolerant digital and analog electronics: Ultra-low power electronics have flown on the NASA ST5 spacecraft and have been developed for the GeoSTAR⁶ correlator. Such components would have a broad applicability to all aspects of future space missions.

Autonomous low-power generation: The DALI concept requires power generation at stations, while the LARC concept requires power generation at each STANCE. More efficient power generation and storage would have applicability to a suite of small satellite missions (micro-sats, cube-sats), as well as potentially to planetary or deep space missions.

Low-mass, high-capability, autonomous rovers: The LRA requires rovers for deployment. Rovers are also applicable to planetary missions (e.g., Mars), industries operating in human-hazard conditions (e.g., interior of nuclear power plants), and the DoD (e.g., DARPA Urban Challenge program).

High data rate, lunar surface data transport: The LRA requires data transport between the science antennas and the central processing facility. High data rate transport would also be required for satellite constellations or terrestrial sensor webs.

⁶ A microwave radiometer for Earth remote sensing.

Lunar Radio Array

Table 3. Key LRA Technology Development

Technology	Requirement	Current State	Required	Heritage	Synergies
Low frequency, wide bandwidth, low-mass science antennas	<ul style="list-style-type: none"> • ~ 20 – 150 MHz • Easy deployment • Minimal mass, volume 	DALI: proof-of-concept antenna LARC: helical antenna concept design	<ul style="list-style-type: none"> • Prototype • Deployment demonstration 	Ground-based radio astronomical arrays	NASA heliophysics missions
Ultra-low power, ultra-low noise, radiation tolerant digital and analog electronics	<ul style="list-style-type: none"> • Low power budgets • Analog amplifiers, ADCs • Digital components • Operate in lunar thermal extremes 	<ul style="list-style-type: none"> • 130 nm process • ~ 1.3 V supply • Primary focus on digital • Limited temp. range 	<ul style="list-style-type: none"> • 12 nm process or better • < 1 V supply • General purpose chips and components 	NASA ST5 spacecraft, GeoSTAR correlator	NASA missions, DoD, commercial
Autonomous low-power generation and storage	<ul style="list-style-type: none"> • 100s to 10,000s of individual station sinks • ~ 0.1 W through lunar night • < 1 kg per station 	<i>Batteries:</i> Best Li-ion ~3 kg/W for 300 hr; must charge at 270 K < T < 310 K	<ul style="list-style-type: none"> • < 1 kg/W • Steady 0.1 W for 300 hr at 100 K • Charge > 310 K 	Planetary spacecraft, rovers	NASA micro-sat missions, small lunar payloads, commercial micro-sats
		<i>RPU:</i> Available > 10 W or < 10 mW	<ul style="list-style-type: none"> • ~ 0.1 W units • Sufficient ²³⁸Pu? 	Multiple deep-space missions	
		<i>Power beaming:</i> Terrestrial system studies	Lunar infrastructure, ~ 10x efficiency		
Low-mass, high capability rovers (DALI only)	<ul style="list-style-type: none"> • High payload / rover mass ratio • Autonomous navigation, antenna deployment 	<ul style="list-style-type: none"> • ~ 850 kg • kW power • Payload / rover mass ratio ~ 3 • 10 cm/s 	<ul style="list-style-type: none"> • 10s of kg • ~ 100 W power • Payload / rover mass ratio ~ 5 • > 1 m/s 	Mars rovers, ATHLETE, DARPA competitions	NASA planetary, lunar exploration; DoD; commercial (human-hazard activities)
High data rate, lunar surface data transport	<ul style="list-style-type: none"> • > 400 Mbps (DALI); > 3 Gbps (LARC) • Low mass • Low power • Operate in lunar thermal extremes • No RFI generating (ITU compliant) 	<i>Free-space laser</i> 10 Mbps	<i>Free-space laser</i> > 400 Mbps	NRL-JPL demonstrations	NASA lunar exploration, satellite constellations
		<i>RF wireless</i> 600 Mbps	<i>RF wireless</i> Non-RFI generating	Commercial RF wireless	
		<i>Optical fiber</i> 1 kg/km	<i>Optical fiber</i> 0.1 kg/km	Commercial optical fiber	

3.2 The Dark Ages Lunar Interferometer (DALI) Concept

The DALI concept is a hierarchical array, based on simple dipole or bowtie-like science antennas deposited on long strips of polyimide film (e.g., Kapton™). The motivation for this approach is two-fold.

1. Both the hierarchical architecture and the antenna topology (dipole or bowtie) have considerable heritage from radio astronomy community. Many of the ground-based radio astronomy interferometers, either existing or under construction, use similar topologies for their science antennas and have similar hierarchical architectures.
2. Space-qualified Kapton has been used in many spacecraft applications and represents a promising low-mass substrate for a science antenna. Even simple estimates suggest that the collecting area for pre-EoR and Dark Ages studies will require thousands of science antennas, so that mass is likely to be a significant driver for the system design.

The hierarchical architecture for DALI consists of individual science antennas, which are grouped into “stations,” which form the overall array (Figure 4). In the current design, there are approximately 1500 science antennas per station and 300 stations in the full array.

A science antenna consists of two crossed, single polarization, dipoles or bowties deposited on polyimide film. The dipoles are entirely passive and nominal film dimensions are 100 m × 1.5 m × 20 μm. The film is flexible enough to be stored in a roll during transit and unrolled directly onto the lunar surface. Dust is not an issue for these antennas—it is an excellent thermal insulator and a thin coating could provide some protection from exposure.

We have conducted two tests of the DALI antenna concept. The first test was a measurement of the feed point impedance of a polyimide-film based antenna. This test was conducted to verify that our simulations of the antenna concept were accurate and did not involve excessive extrapolations of modeling software. The test consisted of a single antenna, two 8-m long segments each 30.5 cm wide, and composed of a 25 μm-thick Kapton with a 5 μm-thick Cu layer deposited on it. The feed point impedance was measured via a network analyzer, and the test was conducted at NASA/GSFC. The test scenario was simulated using the CST Microwave Studio 3D package, with various estimates of the ground characteristics at the NASA/GSFC site. The simulations were not complete, e.g., the ground was only modeled to a depth of 15 m. Nonetheless, the agreement between simulation and measurement is considerable.

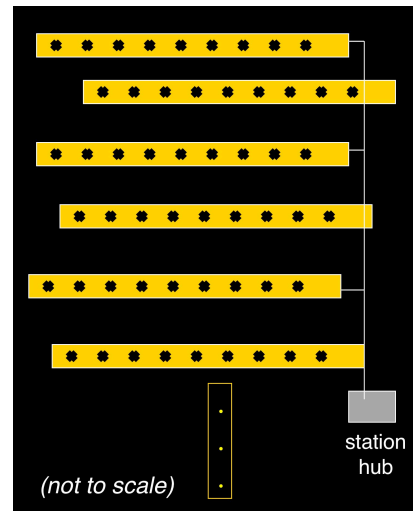


Figure 4. (Left) A prototype polyimide film antenna deployed at NASA/GSFC for feed-point impedance testing. **(Right)** An artist’s conception of a station. Black crosses represent the science antennas and yellow strips represent the polyimide film. The distribution of science antennas within the station is likely to be somewhat more random than illustrated here. Only a portion of the full station is shown for clarity.

The second test consisted of exposing a polyimide film sample to a simulated lunar environment. Two space-rated polyimide film samples were acquired, each being a 10 cm diameter circular sample, 8 μm in thickness, with a silver coating on one side. These were placed in a small thermal vacuum chamber with an interior UV lamp. The chamber contained a platform on which a polyimide film sample could rest, and the temperature of the platform could be changed from -150° C to +100° C. The test plan focussed on the large temperature changes and UV exposure encountered over

Lunar Radio Array

the course of a year. The test film was exposed to a total of 12 cycles over the course of 24 days, from hot (100° C) to cold (-150° C) and back to hot, with the sample also exposed to a deuterium lamp while in the hot cycle. After the simulated year exposure to lunar conditions, the film sample was evaluated for tensile strength, electrical conductivity, and flexibility. No change in the film's properties, typically to 5% precision or better, was found.

A secondary motivation for the use of stations is to co-locate antenna electronics and other electrical components in a central "box" for ease of thermal management, power generation, and electromagnetic shielding. Further, the stations are sufficiently large that multiple fields of view ("multi-beaming") must be formed on the sky in order to acquire a sufficient cosmic volume. Within a station, the radio frequency (RF) signals therefore must be transmitted from the science antennas to the station "hub." In the nominal design, the transmission leads to the station hub are also within/on the polyimide film, however, alternate transmission technologies include RF wireless and fiber optics. Further trade studies are needed to identify the optimum technology.

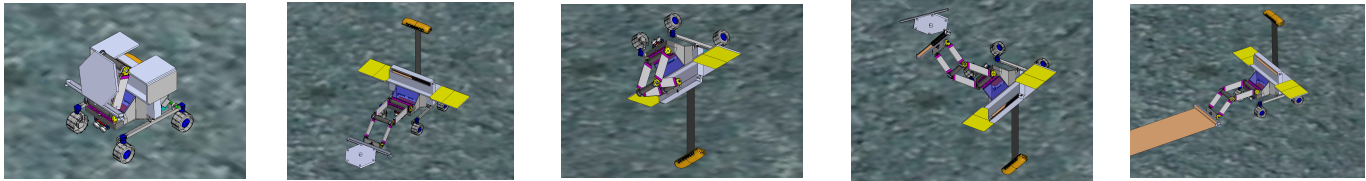


Figure 5. An illustration of part of the station deployment in the DALI concept.

Stations would be deployed by autonomous rovers (Figure 5), and the linear pattern for polyimide film strips shown in Figure 4 would be relatively easy for rover deployment. A uniform distance between polyimide strips is neither required nor desirable, as that would produce "grating lobes" in the station response. The effect of such grating lobes would be to make the calibration of the array more difficult. Thus, it would be acceptable for rovers to shift the deployment locations of polyimide strips by small amounts in order to avoid local features (e.g., small boulders). Further trade studies include the number of stations that a rover would deploy. Options include one rover per station, one rover deploys multiple stations, or a hybrid approach in which multiple stations near the array center are deployed by a single rover while distant stations are each deployed by a rover.

3.3 The Lunar Array for Radio Cosmology (LARC) Concept

The LARC concept (Lunar Array for Radio Cosmology) combines three helical antennas into a single, autonomous phased-array element called a STANCE (Self-Tending Array Node and Communication Element). Preliminary results from trade studies indicate that the number of STANCES needed for the LARC concept to be in the thousands. Given the sheer number of antennas, the following design considerations were implemented:

- Low Mass/Low Volume — antenna mass is the largest driver in the system;
- Autonomy — each STANCE is self-operable and will not impact array performance upon failure; and
- Ease of Deployment — each STANCE is self-deployable and will not require assembly.

Figure 6 illustrates the fully deployed configuration. Each helix is 1.2 m in diameter and attached to a hexagonal plate at its base. The fully-extended helix is 8.2 m high and supported by three vertical scissors-type truss assemblies (not shown). The ten-turn helices are separated by 1.8 m to meet the requirements for effective aperture and field-of-view. The antennas on a given STANCE are all sensitive to the same E-field polarization and are rotated such that the combined power results in a beam pattern, also shown in Figure 6, that has a high degree of circular symmetry. The central hexagon of the STANCE serves as a platform for the electronics canister, the DC power source, and the communications tower. Found inside the electronics canister are the low noise amplifiers, analog-to-digital converters, and digital signal processing unit.

Lunar Radio Array

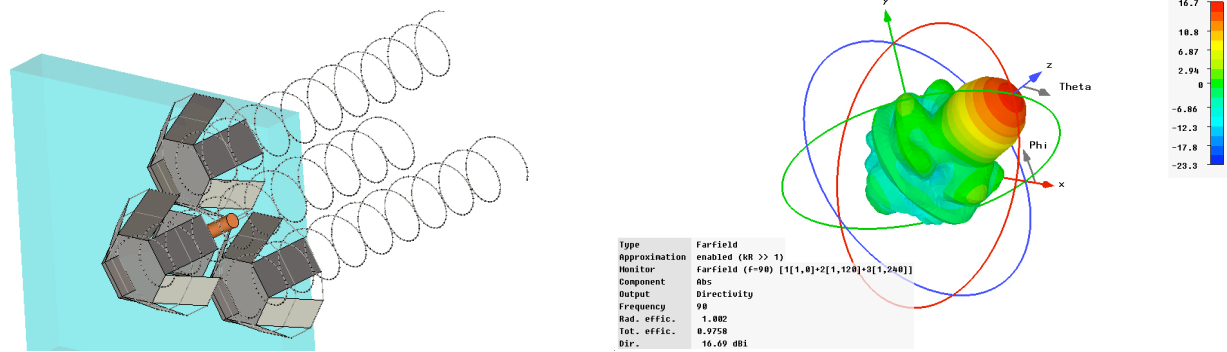


Figure 6. The STANCE concept. (Left) Sketch of the fully deployed configuration (support structure not shown). (Right) Simulated three-dimensional beam pattern at 90 MHz, calculated with CST Microwave Studio software.

Each STANCE’s digital signal processing unit includes a polyphase filter bank that selects the 16 MHz band, trims the data to 4-bit complex samples and packetizes the header information. The packets are passed to a laser transmitter that transmits the data to the central correlator, possibly via local communications nodes. Each laser will be pointed mechanically in azimuth and elevation, and at the receiving station the optical signal will be focused onto arrays of avalanche photodiode detectors. The data rate transmitted to the correlator for each STANCE is 128 Mbs. We estimate that each STANCE will consume about 100 mW. Development of power storage technology appropriate for many of these small autonomous units on the Moon is critical.

While the final number of STANCES will depend on the outcome of further trade studies, we adopt 10,000 LARC STANCES, 5000 of each polarization, as a target. The total data rate to the correlator is over 1 Tb/s. To carry out complex correlation of all polarization products, over 40,000 Tops/sec are required. Scaling this computation load to the current performance of the GeoSTAR correlator⁸ implies that only 200 W of power will be required for the correlator. While the complexity of such a large correlator is a concern, already the remarkable advances in space-qualified ultra-low-power digital electronics enable the processing required for the large antenna array envisioned for the LARC concept.

STANCE deployment has been designed with the objective to eliminate low-mass rover and robotic technology development specific to the LRA. The ATHLETE system (funded by the Constellation Program) will be used both to offload the STANCES from the Altair lander or similar vehicle and place them on the lunar surface. STANCES will be loaded onto a cargo pallet on top of the Altair (Figure 7). After landing, the ATHLETE will unfold its legs, swing them down on the surface, extend and lift the cargo pallet, and “walk off” of the Altair to the deployment site. The ATHLETE will then use two of its legs to reach up, “grab” STANCES using leg attachments, and lower them onto the surface. Once a STANCE has been placed, the ATHLETE will trigger its deployment mechanism.

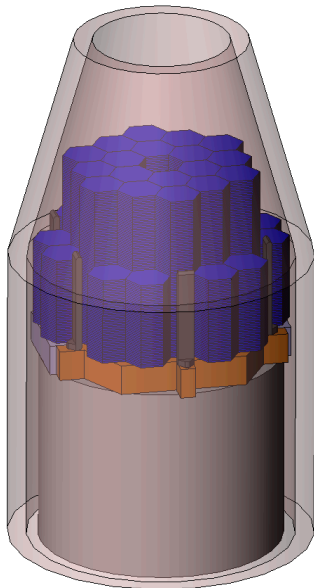


Figure 7. STANCE Packaging

Each STANCE in its packaged state is a single hexagonal plate consisting of four spring-loaded layers. When the deployment mechanism is triggered, three of the layers (the helical antennas) will unfold sequentially from a central hexagon. A communications tower will deploy from the center and establish a communications link. Cavity walls for each helical antenna will unfold “accordion-style” similar to solar panel deployment on ISS. Finally, the helical antennas will deploy to full extension by means of truss structures.

While optimal path planning will be used for actual deployment, current estimates for concentric circle and logarithmic spiral deployment indicate that on the order of a thousand STANCES can be placed by an ATHLETE within a lunar day.

3.4 Roadmap and Precursor Missions

Many ground-based radio arrays have been preceded by prototypes having a smaller number of antennas, but which were scientifically productive themselves, and scientific observations began with many of the ground-based arrays well before they reached their final complement of antennas.

A strawman illustration of the staged deployment of lunar radio interferometers follows. We do not discuss ground-based arrays here, but they provide important scientific pathfinding. Also, we illustrate a potential prime science mission, but each stage also could be used as a technological demonstrator.

Stage I: One dipole (or a few) deployed on the near side or on a lunar orbiter. Key science would be searching for the global signature from the Epoch of the First Stars or probing the lunar ionosphere. A single dipole on the lunar surface could be deployed in a sortie scenario; an example would be the Lunar Array Precursor Station (LAPS), a concept developed under the Lunar Sortie Science Opportunities (LSSO) program. A lunar orbiter could include a single dipole as part of the science payload.

Stage II: A small interferometer located on the near side. Key science would include particle acceleration in the inner heliosphere, and possibly in astrophysical sources. A target number of antennas is 100, which could be deployed in a sortie scenario. Deployment could be done either robotically or with astronaut assistance; an example would be the Radio Observatory for Lunar Sortie Science (ROLSS), a concept developed under the LSSO program.

Stage III: A modest-sized interferometer, possibly located on the far side of the Moon. Such an interferometer would be capable of verifying ground-based observations of the Epoch of Reionization and potentially capable of detecting the magnetospheric emission from brightest extrasolar planets. A target number of antennas is 10^3 . Deployment would be largely robotic, though possibly with astronaut oversight.

Stage IV: A fully capable interferometer located on the far side. Such an instrument would be capable of imaging tomography at least of the Epoch of Reionization and ideally deep into the Dark Ages. A target number of antennas is 10^4 , with deployment conducted robotically.

4 THE LUNAR UNIVERSITY NETWORK FOR ASTROPHYSICS RESEARCH (LUNAR)

Science and technology development for the LRA are currently being conducted in the Lunar University Network for Astrophysics Research (LUNAR), one of the inaugural seven teams in the recently instituted NASA Lunar Science Institute (NLSI). LUNAR consists of 19 institutions, including universities, NASA Centers, Federal laboratories, and the National Radio Astronomy Observatory (PI: J. Burns). LUNAR work will begin in the second half of FY09 and continue for 4 years. A key project in the LUNAR work is Low Frequency Astrophysics & Cosmology, involving

1. Development and refinement of theoretical tools for predicting and analyzing H I signals from the Dark Ages and Epoch of Reionization;
2. Array concept and algorithm development to test configurations and data analysis on existing data sets;
3. Science antenna technology development, including development and deployment of proof-of-concept antennas and stations.

The Low Frequency Cosmology & Astrophysics work within the LUNAR team in turn builds upon three design studies conducted over the past three years:

- **Radio Observatory for Lunar Sortie Science (ROLSS; PI: J. Lazio)**, funded by Lunar Sortie Science Opportunities (LSSO) program, ROLSS would be a near-side precursor mission for the LRA.
- **Dark Ages Lunar Interferometer (PI: J. Lazio)**, funded by the Astrophysics Strategic Mission Concept Studies program.
- **Lunar Array for Radio Cosmology (PI: J. Hewitt)**, funded by the ASMCS program.

ACKNOWLEDGEMENTS

A portion of this work was performed at the Jet Propulsion Laboratory, California Institute of Technology, under a contract with NASA.

Lunar Radio Array

REFERENCES

- [1] Alexander, J. K., and Kaiser, M. L. 1976, JGR, 81, 5948
- [2] Bowman, J. D., Rogers, A. E. E., and Hewitt, J. N. 2008, ApJ, 676, 1
- [3] Cohen, A. S., Lane, W. M., Cotton, W. D., et al. 2007, AJ, 134, 124
- [4] Colless, M., Dalton, G., Maddox, S., et al. 2001, MNRAS, 328, 1039
- [5] Eisenstein, D. J., Zehavi, I., Hogg, D. W., et al. 2005, ApJ, 633, 560
- [6] Furlanetto, S. R., Oh, S. P., and Briggs, F. H. 2006, Phys. Reports, 433, 181
- [7] Komatsu, E., Dunkley, J., Nolta, M. R., et al. 2009, ApJS, 180, 330
- [8] Lambrigsten, B. 2006, "GeoSTAR: Developing a New Payload for GOES satellites," *Proceedings of the 2006 Aerospace Conference*, IEEE
- [9] Loeb, A., and Zaldarriaga, M. 2004, Phys. Rev. Lett., 92, 211301
- [10] Perlmutter, S., Aldering, G., della Valle, M., et al. 1998, Nature, 391, 51
- [11] Pritchard, J. R., and Loeb, A. 2008, Phys. Rev. D, 78, 103511
- [12] Riess, A. G., Filippenko, A. V., Challis, P., et al. 1998, AJ, 116, 1009